



Bacterial inactivation kinetics of a photo-disinfection system using novel titania-impregnated kaolinite photocatalyst

Meng Nan Chong^{a,b,c}, Bo Jin^{b,c,d,*}, Christopher P. Saint^{c,d}

^a CSIRO Land and Water, Ecosciences Precinct, Dutton Park, Queensland 4102, Australia

^b School of Chemical Engineering, The University of Adelaide, 5005 Adelaide, Australia

^c Schools of Earth and Environmental Sciences, The University of Adelaide, 5005 Adelaide, Australia

^d Australian Water Quality Centre, South Australian Water Corporation, 5000 Adelaide, South Australia, Australia

ARTICLE INFO

Article history:

Received 5 January 2010

Received in revised form 7 March 2011

Accepted 9 March 2011

Keywords:

TiO₂

Annular slurry reactor

Photo-disinfection

Inactivation kinetics

E. coli

Hom kinetics model

ABSTRACT

We recently developed a novel titania-impregnated kaolinite (TiO₂-K) catalyst and an annular slurry photoreactor (ASP). The present study was to determine the optimal operational factors: TiO₂-K loading, pH, aeration rate, bacterial population and irradiation time, and their impact on disinfection activity and kinetics of a sewage-isolated *Escherichia coli* sp. (ATCC 11775). The inactivation kinetics were evaluated with experimental data and three Hom series empirical models, namely; the Hom model, modified-Hom model and Hom-Power model. The bacterial inactivation rate in the ASP-TiO₂-K system was pH-independent up to pH 7.0. At optimum conditions, 120 min irradiation time was required to achieve 5 bacterial log-reduction units for an average bacterial inoculum size of 8.0×10^6 CFU mL⁻¹. A sigmoid-shape bacterial inactivation profile with strong shoulder and prolonged tailing characteristics was proven. The inactivation kinetic studies revealed that the modified Hom model appeared to be the best empirical model that could represent the disinfection kinetics, with three different inactivation characteristic regions in the ASP-TiO₂-K system.

© 2011 Elsevier B.V. All rights reserved.

1. Introduction

Water disinfection is one of the most important final treatment stages to ensure the water is free of pathogenic microbes that might convey severe waterborne diseases [1]. To date, various chemical disinfection methods such as chlorination and chloramination have been widely practiced. However, it is of wide concern that these disinfection methods have serious environmental drawbacks, as chlorine can react with natural organic matter or dissolved organic carbon to form recalcitrant disinfection by-products (DBPs) [2–5]. Coleman et al. [5] have reported that a low concentration of common DBPs in water, such as haloacetic acid (60 ppb) and trihalomethanes (80 ppb), might cause serious congenital cardiac defects in human beings following prolonged consumption. In addition, poor maintenance of ammonia during chloramination might result in direct nitrification in water which can directly promote algal blooms and treatment costs [6]. For these reasons, various chemical-free water disinfection technologies without the formation of DBPs have become highly sought in recent years.

Among the chemical-free disinfection methods, heterogeneous photocatalysis employing titanium dioxide (TiO₂) has been investigated extensively [7–9]. Photocatalytic water disinfection operates in a semiconductor system, where the TiO₂ particles are mixed with the targeted water being subjected to UV irradiation. When the TiO₂ particles are irradiated by UV light, the photon energy excites the lone electron from its conduction band to valence band to form the electron-hole pairs [10–12]. In the presence of electron scavengers, the availability of the valence band is prolonged with surface-adsorbed hydroxyl groups being oxidized to radicals [13]. These hydroxyl radicals (OH[•]) are primarily responsible for the inactivation and destruction of microorganisms [13]. In the absence of electron scavengers, no photocatalytic reaction occurs due to the rapid recombination of electron-hole pairs. The detailed photochemical reactions on the TiO₂ surface during photocatalysis have been discussed in the literature [14,15].

Since the pioneering work by Matsunaga et al., a number of preliminary photocatalytic disinfection studies have been shown to successfully inactivate various coliforms, viruses, bacteria, cysts, fungi, algae and protozoa [16–19]. Commercial Degussa P25 TiO₂ has been used in most previous studies. Except those studies of Pulgarin and co-workers [11,20,21], very few other case studies of pilot and large scale processes of such photocatalytic disinfection technologies for water treatment were reported. A technical and economic bottle-neck issue associated with photocatalytic

* Corresponding author at: School of Earth and Environmental Sciences, The University of Adelaide, North Terrace Campus, Adelaide, SA 5005, Australia. Tel.: +61 8 8303 7056; fax: +61 8 8303 6222.

E-mail address: bo.jin@adelaide.edu.au (B. Jin).

treatment process using the P25 TiO₂ is the difficulty, and high cost for separating the fine P25 TiO₂ particles (10–30 nm) [22]. Numerous material engineering solutions have been investigated in order to resolve this problem. One of the more prominent solutions is to immobilise the TiO₂ nanoparticles onto an inert carrier to retain its quantum effects, while allowing ease of separation from the treated water stream [23–27]. Different materials have been successfully demonstrated as potential carriers for TiO₂ nanoparticles, such as optical fibres, clay materials and magnetic cores [28–30].

We recently synthesized a novel titania-impregnated kaolinite (TiO₂-K) catalyst, in which nanocrystal TiO₂ (7.0 nm) particles are immobilised onto layered kaolinite clays (3.5 μm). Due to its high photo-oxidation capacity and recoverable characteristics, the TiO₂-K catalyst has been suggested as a promising catalyst for photocatalytic water treatment. Previously, we have examined the photocatalytic activity of the TiO₂-K particles against the degradation of dye molecules and bacteria in a self-designed annular slurry photoreactor (ASP) [11,31,32]. We found that the bacteria are able to regrow after 24 h, but such a phenomenon can be suppressed by promoting the residual disinfectant effect of the catalysts through concurrent photo-Fenton reaction [32]. In this study, the photo-disinfection performance of the TiO₂-K catalyst was tested against a sewage-isolated *Escherichia coli* sp. (ATCC 11775). Bacterial *E. coli* is a common surrogate measure against treatment efficacy. The use of a strain isolated from sewage allows the measurement of disinfection ability of the treatment process against an organism isolated from a natural environment. The effects of operation factors of the ASP system on the irradiation time required to inactivate 5 bacterial log-reduction units were investigated. These include the TiO₂-K loading, pH, aeration rate and bacterial inoculum size. Subsequently, we evaluated the inactivation kinetics using the empirical Hom series models for comparison and modelling of the disinfection system. The Hom series models used were the Hom model, modified Hom model and Hom–Power model.

2. Materials and methods

2.1. Materials

Chemicals employed for the synthesis of TiO₂-K included titanium (IV) butoxide (tetrabutyl orthotitanate, purum grade ≥97% gravimetric, Sigma–Aldrich), absolute ethanol (AR grade, Labserv Pronalys, Australia), nitric acid (AR grade 69 wt%, BDH VWR, England), and raw kaolinite clays (Unimin, South Australia). Hydrochloric acid (Labserv Pronalys, Australia), sodium hydroxide (Analar grade, BDH Chemicals, England), tryptone soy broth media (TSB) (Oxoid, England) and plate count agar (PCA) (Merck, Germany) were prepared to a desired concentration by the addition of Milli-Q water obtained from a Barnstead Nanopure ion exchange water system with 18.2 MΩ-cm resistivity.

2.2. Preparation of titania impregnated kaolinite catalyst

The TiO₂-K catalyst particles were synthesized in accordance with our previously developed method [30]. A modified two step sol-gel method was used, where 25 mL titanium precursor was hydrolysed by 30 mL absolute ethanol. The resultant hydrolysed mixture was then acid-catalysed under controlled nitric acid conditions. In the following step, this catalysed product was heterocoagulated with 10% (w/v) kaolinite suspension at 37 °C under constant stirring. Prior to the heterocoagulation, the kaolinite clays were pre-treated in a series of alkalization and thermal treatments at 750 °C for 1 h. The kaolinite particles were used as the inert carriers for the deposition of titania sol, enabling ease of catalyst particle separation during the water disinfection application. The

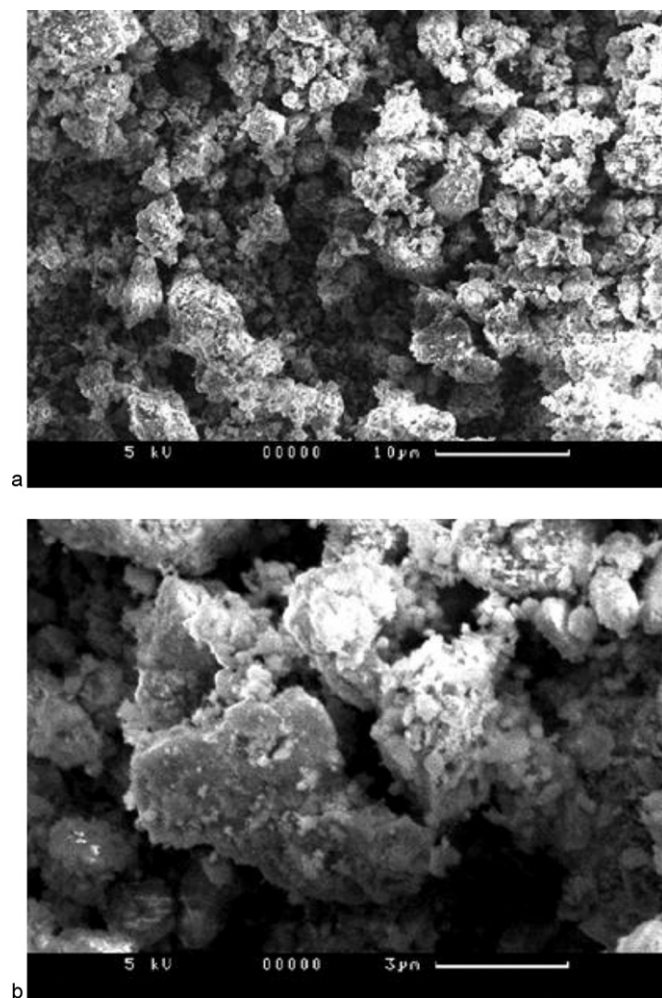


Fig. 1. Scanning electron microscopic images of the TiO₂-K catalyst (a) 10 μm resolution; (b) 3 μm resolution.

heterocoagulated products were filtered and washed repeatedly with distilled water up to three times to remove any excess chemical impurities. The filtrate cake was dried in a conventional oven at 65–70 °C for 3 h, before being fired at 600 °C. Fig. 1 shows the scanning electron microscopic images of the TiO₂-K catalyst at different magnifications.

2.3. Annular slurry photoreactor

In this study, a stainless steel ASP was used as a photo-disinfection reactor [11,31,32]. The ASP was a three-phase bubble column reactor, where the TiO₂-K particles were dispersed in the targeted water via bubble aeration. A detachable conical bottom was made for the ASP to prevent a reaction dead zone for the TiO₂-K catalyst, as well as promoting ease of cleaning and maintenance. At the lower end, a 45-μm air sparger was fitted to provide homogeneous aeration for catalyst suspension and mixing. An UV-A black light of 8 W (NEC, Holland) was positioned annularly within the quartz thimble to prevent direct contact with the reaction fluid, while allowing optimal UV transmission into the annulus reaction zone. The UV-A light was used for photonic excitation of the TiO₂-K catalyst alone. Unlike the germicidal UV-C light with a high-end UV electromagnetic spectrum, the associated UV energy for the UV-A is significantly lower and does not cause substantial direct bacterial inactivation. The wavelength range of UV-A light lies in the range of 315–400 nm, which is close to solar irradiation. The light

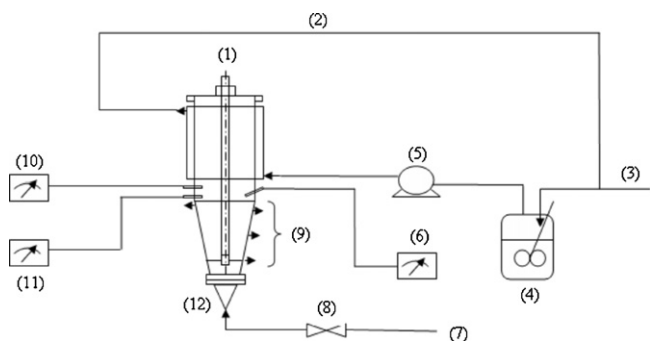


Fig. 2. Experimental set-up for the annular slurry photoreactor system: (1) UV light, (2) recirculation water line, (3) fresh cool water line, (4) cooling water vessel, (5) cooling water pump, (6) temperature meter, (7) compressed air supply line, (8) compressed air regulation valve, (9) sampling ports, (10) pH meter, (11) dissolved oxygen meter, and (12) photoreactor.

intensity in the ASP was measured using a radiometer (Solarmeter[®] SM 5.0 & 8.0, Solartech Inc.). Samples were collected from the four-descended level sampling ports. Electronic probes and meters for in situ data logging of pH, dissolved oxygen and temperature (TPS, Australia) were connected to the reactor. The operating temperature for the ASP system was kept at room temperature of 25 °C during the experiments. The detailed design of the ASP and experimental setup are shown in Fig. 2.

2.4. Cell culture, medium preparation and bacterial counting

To prepare the bacterial suspension, 50 mL fresh liquid culture prepared in TSB was inoculated with the sewage-isolated *E. coli* strain ATCC 11775. The cell culture was incubated in a rotary shaker at 150 rpm and 35 °C for 19 h until the late exponential phase. The cell density during the incubation was determined by heterotrophic plate counts (HPC), and found to be 9×10^9 CFU mL⁻¹ in 19 h. An aliquot of the incubated liquid culture was directly inoculated into 1.5 L of phosphate buffered saline (PBS) solution for bacterial suspension. The use of PBS is to prevent sudden osmotic shock to the bacteria, so as to maintain the bacterial numbers for accurate dilution purposes. The initial bacterial density was also assessed by HPC using standard procedures [33].

Prior to the photo-disinfection experiment, a known amount of TiO₂-K catalyst was mixed to the bacterial suspension and further dark homogenized for 30 min. The UVA light was turned on after the homogenisation period and the bubble aeration was run continuously up to 300 min. Samples were collected every 10 min up to 40 min, thereafter every 20 min up to 120 min, and finally every 60 min up to 300 min. The enumeration of the *E. coli* was carried out following a standard serial dilution procedure and every sample was determined by HPC in the prepared PCA in duplicate. With the duplicate 2.5 mL samples collected from the different sampling ports, a 0.1 mL aliquot was then diluted serially in 0.9 mL PBS. After that, 0.1 mL of each dilution was plated in triplicate to PCA to determine the eventual bacterial cell density. The PCA plates were then incubated at 35 °C for 24 h before final cell counting. The bacterial log-reduction against the irradiation time curve was plotted for kinetic analysis. Each photo-disinfection experiment was then repeated for standard experimental verification and error analysis.

3. Results and discussion

3.1. Effect of TiO₂-K loading

Optimisation of the photocatalyst loading used in a photoreactor system is particularly important, owing to the overall treatment

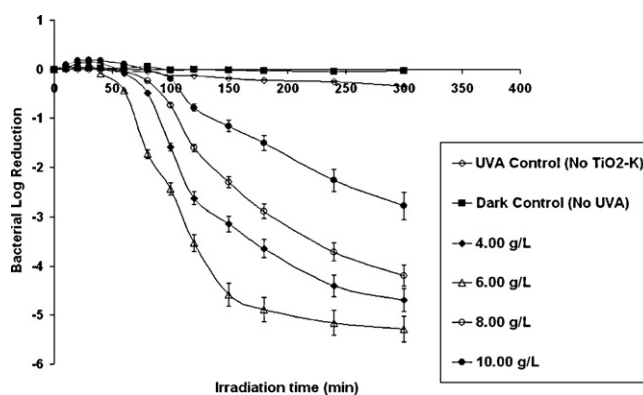


Fig. 3. Effects of TiO₂-K catalyst loadings on the photocatalytic inactivation kinetics of *E. coli* at pH 7.0, 5.0 L min⁻¹ aeration and average initial bacterial population of 8.0×10^6 CFU mL⁻¹.

costs and process efficacy. Previous studies on photocatalyst loadings of the Degussa P-25 TiO₂ on microbial inactivation were reported to be in the range of 0.5–2.0 g L⁻¹, depending on configuration of the photoreactor used [8,17]. In this study, TiO₂-K dosing experiments were studied in a range of 4.0–10.0 g L⁻¹. The overall mass of the TiO₂-K catalyst was mainly contributed by the kaolinite carrier. As previously determined using the zinc oxide spiking method in X-ray diffractionometry, the fractional weight ratio of TiO₂:K is approximately 8% (w/w) [30]. This indicates that the real TiO₂ loading used in this study is approximately 0.30–0.80 g L⁻¹.

Photolysis and dark control experiments were also conducted to measure the net bacterial inactivation level as mediated by different TiO₂-K catalyst loadings. In the UV-A photolytic experiment without TiO₂-K added, it was observed that less than a log bacterial reduction unit was achieved after 300 min of irradiation. This was owing to the fact that UV-A light emits the least energetic fraction of UV spectra (3.10–3.94 eV) that usually cause insignificant damage to the bacterial cell [21]. Rincón et al. [21] reported that photo-killing by UV-A should be well-mediated by sensitizers, such as a TiO₂ catalyst, to achieve greater bacterial cell damage. No inactivation activity was found in the control experiments using TiO₂-K without UV-A irradiation.

When 4.0 g L⁻¹ TiO₂-K was added (Fig. 3), it could be seen that the photo-killing in the ASP was significantly enhanced by approximately thirteen-fold. Such enhancement in bacterial inactivation was due to the formation of reactive oxygen species (ROS) such as OH[•], O₂^{•-} and H₂O₂. Gyürék et al. [34] indicated that the activity of the ROS on the cytoplasmic membrane is cumulative rather than instantly lethal. This is supported by the strong shoulder characteristic in the bacterial inactivation curve, where log-linear bacterial reduction started after 20 min UV-A irradiation. Others were of the view that such prolonged inactivation at the beginning of photocatalyst-mediated disinfection is due to the slow permeation rate of the ROS (i.e., short half-life) through the cell wall [35]. The irradiation time required to achieve approximately 5 log-reduction units was 300 min.

At a high TiO₂-K loading of 6.0 g L⁻¹, however, the strong shoulder characteristics during the bacterial inactivation was found to be depleted. A shorter UV-A irradiation time of 180 min was required to achieve a 5 log bacterial reduction. At an increased TiO₂-K loading of 8.0 g L⁻¹, the bacterial inactivation kinetics becomes more sluggish than for the 6.0 g L⁻¹ loading. Similar attenuation in photo-disinfection efficacy was observed when 10.0 g L⁻¹ of TiO₂-K loading was applied. It is worth noting that further increased TiO₂-K loadings of 8.0 and 10.0 g L⁻¹ resulted in little increase in disinfection efficiency. At a TiO₂-K loading of 10.0 g L⁻¹, for instance, it was impossible to achieve a 5 log bacterial reduction

even at an extended irradiation time. The highest bacterial inactivation levels using 8.0 and 10.0 g L⁻¹ TiO₂-K at pH 7.0 were approximately 4 and 3 log reduction units, respectively. Such attenuation in photo-disinfection efficacy with increasing TiO₂-K loading indicated an increase in the overall light extinction coefficient. At a TiO₂-K particle concentration higher than 6.0 g L⁻¹, the radial light intensity across the annulus width (50 mm) was reduced as a direct result of rapid absorption and scattering by the TiO₂-K particles [12]. As a consequence, the TiO₂-K particles close to the external cell wall were shielded from UV-A excitation and reduced the overall active TiO₂-K in suspension. In this ASP configuration, the overall reaction efficacy is a strong function of the catalyst loading, annulus width and light intensity used. If the light intensity remains unchanged, smaller annulus width can tolerate higher TiO₂-K and vice versa. Considering the ASP operation, it can be concluded that the saturated TiO₂-K loading in the current experimental setup was 6.0 g L⁻¹. All the subsequent investigations will be carried out at such saturated TiO₂-K loading.

3.2. Effect of pH

In a semiconductor photocatalytic system, pH takes a key role in driving the oxidation reaction and efficiency. The pH can affect the surface charge of the photocatalysts used, and subsequently the rate of photooxidation [36–38]. When the pH is higher than the point of zero charge (PZC) of the TiO₂ catalyst, i.e., pH < PZC (TiO₂), the surface of the photocatalyst is positively charged, otherwise it is oppositely charged at pH > PZC (TiO₂). For nominal TiO₂ catalysts, such as the P-25, their PZC usually lies in the range of 5.6–6.8 [37]. However, the PZC of the TiO₂-K particles used was determined to be 9.5 [11]. To investigate the effects of pH in the photo-disinfection of *E. coli* by the TiO₂-K catalyst, a variation of pH 4.0–10.0 was simulated in the ASP system.

E. coli is a Gram-negative bacterium with the outer cell membrane covered by a lipopolysaccharide layer of 1–3 μm thickness [39]. With the slightly negatively charged outer *E. coli* surface, it is expected that this bacterium could have an enhanced photo-disinfection rate with a TiO₂-K catalyst at pH < PZC (TiO₂-K). This is owing to the nature of the heterogeneous TiO₂ photocatalytic reaction, where the microbial contaminants transfer to the vicinity of the TiO₂ surface for subsequent cyclic ROS penetration. The pH can affect the surface charge density of the TiO₂-K catalyst, according to the following equilibrium Eqs. (1) and (2) [9];



Fig. 4 illustrates the effect of pH 4.0–10.0 in the ASP on the photo-disinfection of *E. coli*. In this instance, the initial pH was adjusted using 0.1 M sodium hydroxide and hydrochloric acid, respectively. Three control experiments on the direct UV-A photolysis and dark adsorption at both pH 4.0 and 7.0, respectively, were carried out to ensure that the bacterial disinfection was purely mediated by the TiO₂-K photo-disinfection. Similar results of less than 1 log bacterial reduction unit were obtained in the UV-A direct photolysis even when the pH was adjusted to 4.0. These agreed with the findings by Pulgarin and co-workers [9]. They found that the photolytic inactivation of *E. coli* was independent of initial pH between 4.0 and 9.0. A low degree of bacterial reduction was also observed for the dark adsorption at both pH 4.0 and 7.0 without UVA irradiation. In this instance, pH 4.0 was observed to be the optimal value to achieve a maximum disinfection level for the TiO₂-K photocatalysis. Heyde and Portulier [40] explained that the negligible *E. coli* reaction to acid conditions was due to the presence of an acid tolerance response in the bacterium itself, which secreted the acid-induced proteins for bacterial acid-shock protection.

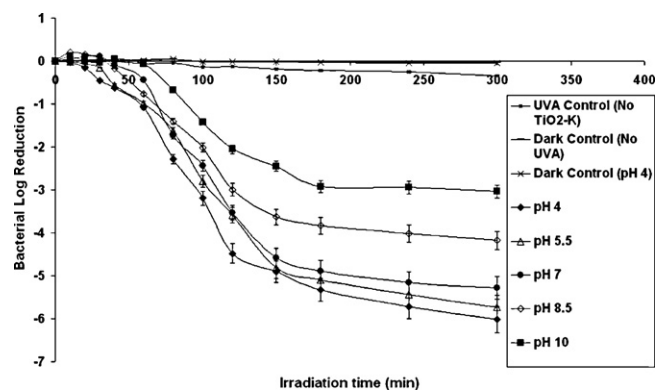


Fig. 4. Effects of pH on the photocatalytic inactivation kinetics of *E. coli* at 6.0 g L⁻¹ TiO₂-K, 5.0 L min⁻¹ aeration and average initial bacterial population of 8.0 × 10⁶ CFU mL⁻¹.

Fig. 4 indicated that a high photo-disinfection rate of *E. coli* was associated with a low pH. This may be attributed to the high proportion of dense TiOH₂⁺ groups formed that draw the *E. coli* to the TiO₂-K surface for the cell destruction process. The total irradiation time required to achieve 5 log-reduction units was shortened to 150 min compared to the experiment at pH 7.0. A declining trend in the photo-disinfection activity of the TiO₂-K was observed at pH up to 10.0. Similarly, the total irradiation time taken to achieve 5 log-reduction units at a pH over 8.5 was prolonged. It was however, interesting to note that the bacterial inactivation during the tailing region was enhanced at a low pH. This was owing to more TiOH₂⁺ groups being generated and thus, increases in the electrostatic attraction force between the TiOH₂⁺ groups and *E. coli*. The photo-disinfection activity was significantly reduced at pH 8.5 and 10, which was very close to PZC (TiO₂-K) = pH 9.5. Completely sluggish photo-disinfection kinetics of *E. coli* were observed at pH 10.0; in particular, the bacterial inactivation during the tailing region, as both TiO₂-K and *E. coli* surfaces become repellent of each other. It was, however, noteworthy to find that the TiO₂-K catalyst with high PZC is highly functional under a wide pH range. Unlike a conventional TiO₂ catalyst with low PZC, it can be concluded that disinfection using the TiO₂-K can be conducted at a wide pH range, and a low pH can lead to a high disinfection rate due to the high electrostatic interaction. Thus, all the subsequent experiments were carried out at pH 4.0 in order to investigate the maximal photo-disinfection activity that could be attained.

3.3. Effect of aeration

In the three phase ASP system, compressed air was used to disperse and keep the TiO₂ catalyst in suspension apart from providing sufficient dissolved oxygen (DO) for electron-hole pair formation [11,31,32]. The extent of aeration used, however, can affect the suspension states of the TiO₂-K particles in the ASP. Two different states of TiO₂-K suspension can exist in the ASP system: homogeneous suspension where the TiO₂-K particles are uniformly distributed throughout the ASP; and heterogeneous suspension in which the TiO₂-K particles are non-uniformly distributed but in complete suspension [11].

To investigate the effect of aeration rate on the photo-disinfection activity of the TiO₂-K-ASP system, a step change in aeration rate from 2.5 L min⁻¹ to 10.0 L min⁻¹ was evaluated (Fig. 5). Previously, the effect of aeration rate on the photodegradation of Congo red dye molecules was investigated [11]. At 2.5 L min⁻¹, we found large sediments of TiO₂-K particles on the sparger plate. This was because a low aeration pressure cannot keep the TiO₂-K particles suspended in the reactor. The

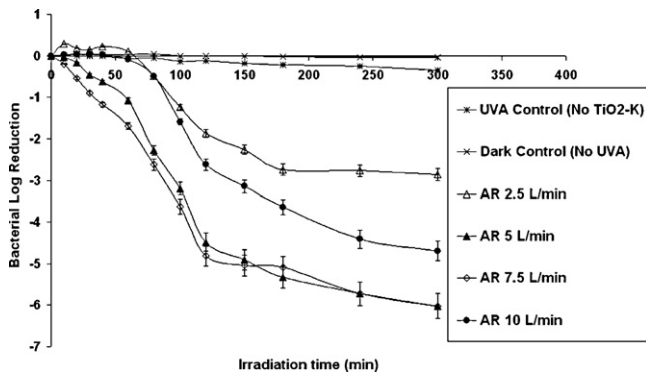


Fig. 5. Effects of delivered aeration rate on the photocatalytic inactivation kinetics of *E. coli* at 6.0 g L^{-1} $\text{TiO}_2\text{-K}$, pH 4.0 and average initial bacterial population of $8.0 \times 10^6 \text{ CFU mL}^{-1}$.

photo-disinfection kinetic profile associated with 2.5 L min^{-1} , was found to exhibit strong shoulder characteristics. Marugán et al. [4] proposed that the appearance of such shoulder characteristics was due to the low volumetric generation rate of ROS. This means that the amount of active $\text{TiO}_2\text{-K}$ in suspension is low, resulting in strong bacterial growth inhibition of the photo-disinfection activity of $\text{TiO}_2\text{-K}$ catalyst.

The overall photo-disinfection rate was lower at 2.5 L min^{-1} than at 5.0 L min^{-1} . This was evidenced from the prolonged irradiation time required to achieve only 3 log-reduction units after 300 min. Our previous experiments showed that the $\text{TiO}_2\text{-K}$ particles could remain in homogeneous suspension in the ASP at 7.5 L min^{-1} . Similarly, the optimal rate obtained in this photo-disinfection study was 7.5 L min^{-1} , where only 120 min was required to achieve a 5 log bacterial reduction. It was interesting to note that the shoulder characteristic disappeared when the ROS volumetric generation rate was high. Thus, it can be verified that shoulder characteristic in disinfection kinetics is a strong function of the ROS volumetric generation rate, which is dependent on the state of the catalyst suspension. A further increase in the aeration (10 L min^{-1}) resulted in a low disinfection rate compared with those at 5.0 and 7.5 L min^{-1} , respectively. Chin et al. [41] reported that a high aeration rate can create turbulence in the reaction water mixture, resulting in a “shadow” effect that attenuates light distribution within the reactor. It can be thus concluded that the optimum aeration was 7.5 L min^{-1} . All the subsequent experiments were aerated at 7.5 L min^{-1} .

3.4. Effect of bacterial population

The number of viable bacteria in different water sources may vary. It is thus practicable to investigate the effect of bacterial population on the photo-disinfection kinetics in the ASP. Dunlop et al. [42] found that the inactivation rate was proportional to the initial bacterial loading that presents in the water. At a high bacterial loading, the probability of collision between the *E. coli* and catalyst used increases and directly reduces the mass transfer rates at the catalyst surface. A similar observation was reported by Pham et al. [43] in their study on *Bacillus pumilus* spores in a slurry reactor.

Fig. 6 shows the effect of the initial bacterial population on the photocatalytic inactivation rate of *E. coli* under optimum conditions. The inactivation rate increased with the bacterial cell loadings from 10^5 to 10^6 CFU mL^{-1} , and thereafter decreased significantly, owing to the effect of increasing bacterial population on the light extinction coefficient. A longer irradiation time was seen to be required at the higher bacterial cell loading. Such observation might be owing to the annulus width of the ASP, where the increase in turbidity (bacterial cell loading) might attenuate the radial light

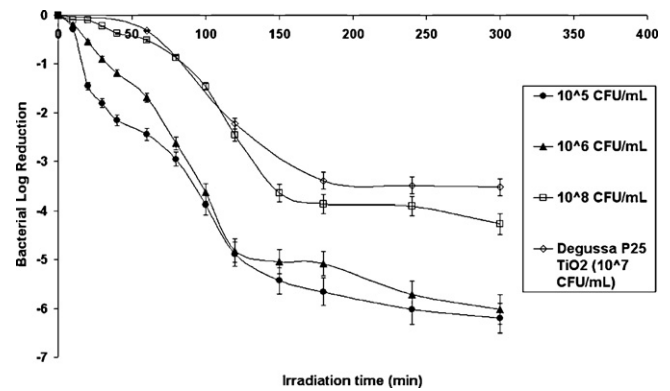


Fig. 6. Effect of initial bacterial population on the photocatalytic inactivation kinetics of *E. coli* under operating conditions of ASP: TNC loading of 6.0 g L^{-1} , pH 4.0 and aeration rate of 7.5 L min^{-1} .

intensity. This was associated with the current annulus width of 50 mm, where the ASP system poses a limitation to a certain range of bacterial loading. From Fig. 6, it was determined that the most viable bacterial loading would be $10^5\text{--}10^8 \text{ CFU mL}^{-1}$. A standard curve of photocatalytic inactivation rate of *E. coli* using 1.0 g L^{-1} of Degussa P-25 TiO_2 was included as a baseline comparison. It should be noted that a conservative TiO_2 concentration of 1.0 g L^{-1} was chosen as a comparison to 6.0 g L^{-1} of $\text{TiO}_2\text{-K}$, as the fractional weight ratio of $\text{TiO}_2\text{:K}$ is approximately 8% (w/w). A direct quantification of the photo-disinfection rate was evaluated in Section 3.5 using the Hom model series.

3.5. Evaluation of empirical models for the photo-disinfection in ASP system

Since the first application of TiO_2 catalysts by Matsunaga et al. [16] for microbial inactivation, most photo-disinfection kinetic modelling works have been based on the Chick–Watson (CW) model [7,35]. In this CW model, the reduction in enumerated bacteria was proportional to the contact time. This correlation, however, cannot be applicable for every instance, as various factors such as the reactor configuration, inactivation mode and the bacterial resistance to disinfectant used might also cause severe non-linearity characteristics. From the previous sections, we found that the photo-disinfection kinetics of *E. coli* by UVA/ $\text{TiO}_2\text{-K}$ yielded non-linear profiles with both shoulders and tailing characteristics. The use of a CT-design concept in the CW model in this instance could “over-simplify” the photo-disinfection rate, resulting in the generation of inaccurate information for design of a photocatalytic disinfection system.

In this section, the applicability of the Hom series models was evaluated for the representation of photo-disinfection kinetics of *E. coli* in the ASP system with three different inactivation characteristics. Mostly, the $\text{TiO}_2\text{-K}$ inactivation profile begins with (i) a lag or initial smooth decay, known as the “shoulder”, followed by (ii) a typical log-linear inactivation region, and ends with (iii) a long deceleration process at the end of the disinfection, which is known as the “tail” [4]. Within the Hom series models, three different Hom-based empirical models – namely, the Hom model, modified-Hom model and Hom–Power model – were compared and evaluated. The difference in the empirical modes is the number of empirical parameters, which directly correspond to the number of non-linearity that occurs within a disinfection profile. In all instances, the photo-disinfection kinetics was assumed to be demand-free, where the photocatalyst loading is constant with contact time.

Table 1Estimated values for the empirical Hom series parameters during the photocatalytic inactivation kinetics of *E. coli* under optimum operational conditions.

Empirical model	k	k_1	k_2	k_3	m	n	x	N_0	Correlation coefficient R^2
Hom	0.0622	–	–	–	0.8792	0.4288	–	–	0.9821
Modified Hom	–	5.7561	0.0288	6.2582	–	–	–	–	0.9904
Hom–Power	3.9687	–	–	–	0.2945	0.9008	1.0009	8.00E+06	0.8117

Hom [44] proposed the empirical Hom model after it was observed that the survivor plots of natural algal–bacterial systems were curvilinear, rather than typical log–linear type (Eq. (3));

$$\log \frac{N}{N_0} = -kC^n T^m \quad (3)$$

where $\log N/N_0 = \log$ bacterial reduction unit; N is the bacterial population at time, t ; N_0 is the initial bacterial population; $k = \text{experimental reaction rate}$; $C = \text{concentration of photocatalyst used}$; T is the applied irradiation time and $m, n = \text{empirical parameters}$. This two-parameter empirical model predicts the bacterial inactivation in a non-linear function for both C and T and is directly dependent on the model parameters n and m , respectively. Owing to the two-parameter nature of the model, it can only account for either shoulder or tailing characteristics but not both. A modification (Eq. (4)) to incorporate an additional empirical parameter was made to accurately account for the three different inactivation characteristics [4,35];

$$\log \frac{N}{N_0} = -k_1 [1 - \exp(-k_2 t)]^{k_3} \quad (4)$$

where k_1, k_2 and k_3 is the empirical constants for the modified Hom model. Similarly, a further modification was modified and integrated according to the Rational Model with the introduction of parameter x to yield the Hom–Power model (Eq. (5)) [45];

$$\log \frac{N}{N_0} = -\frac{\log[1 + N_0^{x-1}(x-1)kC^n T^m]}{(x-1)} \quad (5)$$

where x is the additional empirical parameter for the Hom–Power model. Table 1 shows the evaluation and comparison of the Hom model series for modelling the photo-disinfection activity using the $\text{TiO}_2\text{-K}$ under the optimum condition. All these models were then fitted to the experimental data via a non-linear approach, where the Excel® solver function was used together with the correlation coefficient as an indicator for the degree of fittingness. The outcomes revealed that both the Hom and modified Hom models show a high degree of fittingness, while the Hom–Power model was over-parameterization. These were evidenced from the high correlation to unity by the Pearson correlation coefficient values (R^2). It was found that the Hom model has a limited application under the optimum condition only, where the shoulder characteristic becomes less subtle. The m -value for the Hom model was then estimated to be 0.8792, which only accounted for the tailing region of the *E. coli* inactivation curves. This m -value actually suggested the presence of strong tailing during the disinfection in the ASP system. Similar tailing observation with m -value less than unity was observed by Roy et al. [46] during their ozone inactivation study on poliovirus type 1.

A better fittingness was observed with the modified Hom model under the optimum condition. It was found that the modified Hom model gives a more realistic mathematical expression as it takes into account the three different inactivation characteristics in the kinetic profiles. Marugán et al. [4] have used a similar modified Hom model for the photo-disinfection kinetic modelling of *E. coli* using standard P-25 TiO_2 . By comparison, we found that the $\text{TiO}_2\text{-K}$ used in this study has a comparable photo-disinfection activity but possesses an additional separation edge for possible large-scale

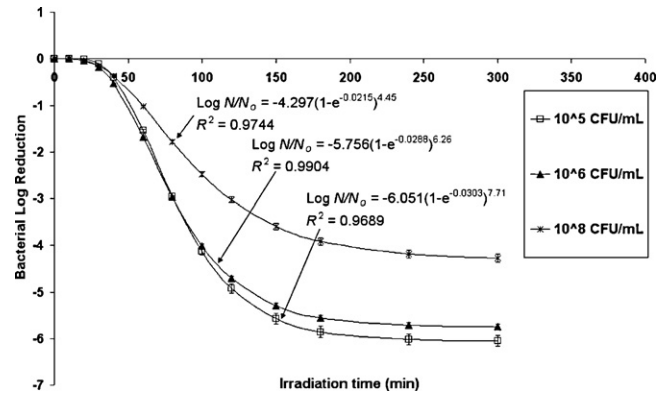


Fig. 7. Fitting of modified Hom model to the photocatalytic inactivation kinetics of *E. coli* for different initial bacterial populations under optimum treatment conditions.

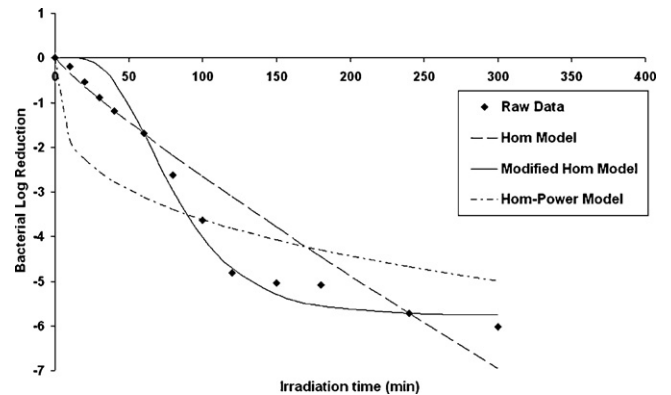


Fig. 8. Comparison of the Hom series model for the fitting of photocatalytic inactivation kinetics of *E. coli* at optimum treatment conditions.

operation. Fig. 7 shows the fitting of the modified Hom model for different bacterial loadings along with its empirically estimated parameters. A low degree of fittingness, however, was observed with the Hom–Power model, when comparing its R^2 value with the other Hom series models. This four-parameter empirical model was found to have logarithmic-constrained inflexion on the bacterial inactivation modelling, to simultaneously represent shoulder and tailing behaviours. A comparison plot on the fitting of the different Hom series models under optimum condition is shown in Fig. 8. Thus, it can be concluded that the modified Hom model provides a more realistic empirical model to account for the non-linear photo-disinfection profiles of *E. coli* in the ASP system.

4. Conclusion

The photo-disinfection kinetics of a sewage-isolated *E. coli* strain (ATCC 11775) using $\text{TiO}_2\text{-K}$ particles as an alternative photocatalyst was successfully demonstrated in this study. Under the illumination of UV-A light, a 5-log bacterial reduction was achieved in 70 min at the optimal operation conditions. The optimal operating conditions for the ASP system were experimentally determined

as 6 g L^{-1} $\text{TiO}_2\text{-K}$ loading, pH 4.0 and 7.5 L min^{-1} aeration rate. It was, however, found that the $\text{TiO}_2\text{-K}$ catalyst was operable under a wider span of pH conditions, of up to pH 7.0 when compared to other conventional photocatalysts. A very low photo-disinfection rate was given at pH 10.0, which is related to the surface charge alteration of PZC ($\text{TiO}_2\text{-K}$) that weakens the *E. coli* interaction link. All disinfection experiments demonstrated a highly non-linear bacterial inactivation kinetic profile, which started with shoulder lag, log-linear bacterial deactivation and prolonged tailing. The shoulder characteristic was strongly influenced by both the optimal $\text{TiO}_2\text{-K}$ dosing and homogeneous dispersion. Subsequent evaluation on the aptness of the Hom series model in representing the photo-disinfection of the $\text{TiO}_2\text{-K}$ catalyst in the ASP found that the modified Hom model is the best empirical model. Both the Hom and Hom-Power model were seen to under and over-parameterize the kinetic profiles with three different inactivation regions. From this study, it is anticipated that the ASP- $\text{TiO}_2\text{-K}$ system could be applied as an alternative disinfection method to replace the current chemical disinfectant methods in the water industry.

Acknowledgement

The authors would like to thank Ms. Vipasiri Vimonses and Mr. Mats Drews for their assistance during the study. This work was funded by the Australian Research Council Linkage Grant (LP0562153) and the Australian Water Quality Centre, SA Water Corporation through the Water Environmental Biotechnology Laboratory (WEBL) at the University of Adelaide, Australia.

References

- [1] D.D. Sun, J.H. Tay, K.M. Tan, Photocatalytic degradation of *E. coli* form in water, *Water Research* 37 (2003) 3452–3462.
- [2] H. Yang, H. Cheng, Controlling nitrite level in drinking water by chlorination and chloramination, *Separation and Purification Technology* 56 (2007) 392–396.
- [3] J. Lu, T. Zhang, J. Ma, Z. Chen, Evaluation of disinfection by-products formation during chlorination and chloramination of dissolved natural organic matter fractions isolated from a filtered river water, *Journal of Hazardous Materials* 162 (2009) 140–145.
- [4] J. Marugán, R.V. Grieken, C. Sordo, C. Cruz, Kinetics of the photocatalytic disinfection of *Escherichia coli* suspensions, *Applied Catalysis B: Environmental* 82 (2008) 27–36.
- [5] H.M. Coleman, C.P. Marquis, J.A. Scott, S.S. Chin, R. Amal, Degradation of 1,4-dioxane in water using TiO_2 based photocatalytic and $\text{H}_2\text{O}_2/\text{UV}$ processes, *Chemical Engineering Journal* 113 (2005) 55–63.
- [6] A. Sathasivan, I. Fisher, T. Tam, Onset of severe nitrification in mildly nitrifying bulk waters and its relation to biostability, *Water Research* 42 (2008) 3623–3632.
- [7] M. Cho, H. Chung, W. Choi, J. Yoon, Linear correlation between inactivation of *E. coli* and OH radical concentration in TiO_2 photocatalytic disinfection, *Water Research* 38 (2004) 1069–1077.
- [8] A.G. Rincón, C. Pulgarin, Photocatalytic inactivation of *E. coli*: effect of (continuous - intermittent) light intensity and of (suspended - fixed) TiO_2 concentration, *Applied Catalysis B: Environmental* 44 (2003) 263–284.
- [9] A.G. Rincón, C. Pulgarin, Effect of pH, inorganic ions, organic matter and H_2O_2 on *E. coli* K12 photocatalytic inactivation by TiO_2 : Implications in solar water disinfection, *Applied Catalysis B: Environmental* 51 (2004) 283–302.
- [10] L. Rizzo, J. Koch, V. Belgiorno, M.A. Anderson, Removal of methylene blue in a photocatalytic reactor using polymethylmethacrylate supported TiO_2 nanofilm, *Desalination* 211 (2007) 1–9.
- [11] M.N. Chong, S. Lei, B. Jin, C. Saint, C.W.K. Chow, Optimisation of an annular photoreactor process for degradation of Congo Red using a newly synthesized titania impregnated kaolinite nano-photocatalyst, *Separation and Purification Technology* 67 (2009) 355–363.
- [12] I.J. Ochuma, R.P. Fishwick, J. Wood, J.M. Winterbottom, Optimisation of degradation conditions of 1,8-diazabicyclo[5.4.0]undec-7-ene in water and reaction kinetics analysis using a concurrent downflow contactor photocatalytic reactor, *Applied Catalysis B: Environmental* 73 (2007) 259–268.
- [13] J.M. Herrmann, Heterogeneous photocatalysis: fundamentals and applications to the removal of various types of aqueous pollutants, *Catalysis Today* 53 (1999) 115–129.
- [14] I.K. Konstantinou, T.A. Albanis, TiO_2 -assisted photocatalytic degradation of azo dyes in aqueous solution: kinetic and mechanistic investigations: A review, *Applied Catalysis B: Environmental* 49 (2004) 1–14.
- [15] R.J. Watts, S. Kong, W. Lee, Sedimentation and reuse of titanium dioxide: Application to suspended-photocatalyst reactors, *Journal of Environmental Engineering* 121 (1995) 730–735.
- [16] T. Matsunaga, R. Tomodam, T. Nakajima, H. Wake, Photoelectrochemical sterilization of microbial cells by semiconductor powders, *FEMS Microbiology Letters* 29 (1985) 211–214.
- [17] E.J. Wolfrum, J. Huang, D.M. Blake, P.C. Maness, Z. Huang, J. Fiest, Photocatalytic oxidation of bacteria, bacterial and fungal spores, and model biofilm components to carbon dioxide on titanium dioxide-coated surfaces, *Environmental Science and Technology* 36 (2002) 3412–3419.
- [18] J. Hong, M. Otaki, Effects of photocatalysis on biological decolorization reactor and biological activity of isolated photosynthetic bacteria, *Journal of Bioscience and Bioengineering* 96 (2003) 298–303.
- [19] J.A. Ibáñez, M.I. Litter, R.A. Pizarro, Photocatalytic bactericidal effect of TiO_2 on *Enterobacter cloacae*: Comparative study with other Gram (-) bacteria, *Journal of Photochemistry and Photobiology A: Chemistry* 157 (2003) 81–85.
- [20] A.G. Rincón, C. Pulgarin, Use of coaxial photocatalytic reactor (CAPHORE) in the TiO_2 photo-assisted treatment of mixed *E. coli* and *Bacillus* sp. and bacterial community present in wastewater, *Catalysis Today* 101 (2005) 331–344.
- [21] A.G. Rincón, C. Pulgarin, Comparative evaluation of Fe^{3+} and TiO_2 photo-assisted processes in solar photocatalytic disinfection of water, *Applied Catalysis B: Environmental* 63 (2006) 222–231.
- [22] Z. Ding, H.Y. Zhu, G.Q. Lu, P.F. Greenfield, Photocatalytic properties of titania pillared clays by different drying methods, *Journal of Colloids and Interface Science* 209 (1998) 193–199.
- [23] J. Fernandez, J. Kiwi, J. Baeza, J. Freer, C. Lizama, H.D. Mansilla, Orange II photocatalysis on immobilised TiO_2 : Effect of the pH and H_2O_2 , *Applied Catalysis B: Environmental* 48 (2004) 205–211.
- [24] K. Mogyorosi, I. Dekany, J.H. Fendler, Preparation and characterization of clay mineral intercalated titanium dioxide nanoparticles, *Langmuir* 19 (2003) 2938–2946.
- [25] R. Molinari, F. Pirillo, M. Falco, V. Loddo, L. Palmisano, Photocatalytic degradation of dyes by using a membrane reactor, *Chemical Engineering and Processing* 43 (2004) 1103–1114.
- [26] Z. Xiong, Y. Xu, L. Zhu, J. Zhao, Enhanced photodegradation of 2,4,6-trichlorophenol over palladium phthalocyaninesulfonate modified organobentonite, *Langmuir* 21 (2005) 10602–10607.
- [27] W. Yan, B. Chen, S.M. Mahurin, E.W. Hagaman, S. Dai, H. Overbury, Surface sol-gel modification of mesoporous silica materials with TiO_2 for the assembly of ultrasmall gold nanoparticles, *Journal of Physical Chemistry B* 108 (2004) 2793–2796.
- [28] D. Beydoun, R. Amal, Implications of heat treatment on the properties of a magnetic iron oxide-titanium dioxide photocatalyst, *Material Science and Engineering B* 94 (2002) 71–81.
- [29] S. Takeda, S. Suzuki, H. Odaka, H. Hosono, Photocatalytic TiO_2 thin film deposited onto glass by DC magnetron sputtering, *Thin Solid Films* 392 (2001) 338–344.
- [30] M.N. Chong, V. Vimonses, S. Lei, B. Jin, C. Chow, C. Saint, Synthesis and characterisation of novel titania impregnated kaolinite nano-photocatalyst, *Microporous and Mesoporous Materials* 117 (2009) 233–242.
- [31] M.N. Chong, B. Jin, C. Chow, C. Saint, A new approach to optimise an annular slurry photoreactor system for the degradation of Congo Red: statistical analysis and modelling, *Chemical Engineering Journal* 152 (2009) 158–166.
- [32] M.N. Chong, B. Jin, H. Zhu, C. Saint, Bacterial inactivation kinetics, regrowth and synergistic competition in a photocatalytic disinfection system using anatase titanate nanofiber catalyst, *Journal of Photochemistry and Photobiology A: Chemistry* 214 (2010) 1–9.
- [33] APHA, Standard Methods for the Examination of Water and Wastewater, 21st edition, 2005.
- [34] L.L. Gyürék, G.R. Finch, Modelling water treatment chemical disinfection kinetics, *Journal of Environmental Engineering* 124 (1998) 783–792.
- [35] M. Cho, H. Chung, J. Yoon, Disinfection of water containing natural organic matter by using ozone-initiated radical reactions, *Applied Environmental Microbiology* 69 (2003) 2284–2291.
- [36] C.S. Zalazar, C.A. Martin, A.E. Cassano, Photocatalytic intrinsic reaction kinetics. II: effects of oxygen concentration on the kinetics of the photocatalytic degradation of dichloroacetic acid, *Chemical Engineering Science* 60 (2005) 4311–4322.
- [37] A.P. Toor, A. Verma, C.K. Jotshi, P.K. Bajpai, V. Singh, Photocatalytic degradation of Direct Yellow 12 dye using UV/ TiO_2 in a shallow pond slurry reactor, *Dyes and Pigments* 68 (2006) 53–60.
- [38] Q. Chang, H. He, Z. Ma, Efficient disinfection of *Escherichia coli* in water by silver loaded alumina, *Journal of Inorganic Biochemistry* 102 (2008) 1736–1742.
- [39] R. Sonohara, N. Muramatsu, H. Ohshima, T. Kondo, Difference in surface properties between *Escherichia coli* and *Staphylococcus aureus* as revealed by electrophoretic mobility measurements, *Biophysical Chemistry* 55 (1995) 273–277.
- [40] M. Heyde, R. Portalier, Acid shock proteins of *Escherichia coli*, *FEMS Microbiology Letters* 69 (1990) 19.
- [41] S.S. Chin, T.M. Lim, K. Chiang, A.G. Fane, Factors affecting the performance of a low-pressure submerged membrane photocatalytic reactor, *Chemical Engineering Journal* 130 (2007) 53–63.
- [42] P.S.M. Dunlop, J.A. Byrne, N. Manga, B.R. Eggs, The photocatalytic removal of bacterial pollutants from drinking water, *Journal of Photochemistry and Photobiology A: Chemistry* 148 (2002) 355–363.

- [43] H.N. Pham, T. McDowell, E. Wilkins, Quantitative analysis of variations in initial bacillus pumilus spore density in aqueous TiO₂ suspension and design of a photocatalytic reactor, *Journal of Environmental Science and Health A* 30 (1995) 627–636.
- [44] L.W. Hom, Kinetics of chlorine disinfection in an ecosystem, *Journal of Sanitary Engineering Division* 98 (1972) 183–194.
- [45] J. Anotai, Effect of calcium ions on chemistry and disinfection efficiency of free chlorine at pH 10, PhD dissertation, Drexel University, Philadelphia, PA (1996).
- [46] D. Roy, E.S.K. Chian, R.S. Engelbrecht, Kinetics of enteroviral inactivation by ozone, *Journal of Environmental Engineering Division ASCE* 107 (1981) 887–901.